Direct Measurement of the Dependence on Electron Density of the Recombination-Rate Coefficient of He_2^+ with Electrons in a High-Pressure Helium Plasma*

C. B. Collins, H. S. Hicks, and W. E. Wells
University of Texas, Dallas, Texas 75230
(Received 9 February 1970)

A computer-linked spectroscopic system with a high-sensitivity-resolution product has been used to measure the time-dependent net rate of production of neutral helium molecules resulting from the recombination of He_2^+ with electrons in a pulsed helium afterglow at a neutral pressure of 44.6 Torr. The relative recombination-rate cofficient of He_2^+ as a function of afterglow time has been obtained by dividing these data by the unscaled product of the electron and molecular ion density as determined from levels in Saha equilibrium with the free electrons. Simultaneous measurement of the electron density with a 35-Gc/sec microwave interferometer has given the unscaled rate coefficient as a continuous function of electron density over the range 10^{10}–10^{12} cm^{-3} without the need of *a priori* assumptions about the functional form. Scale has been established through integration of the rate equation for the loss of ions. Empirically, the rate coefficient can be represented as $\alpha = 2.8 \times 10^{-11}[e]^{0.185}$ cm^3/sec, where e is the electron density in cm^{-3}.

INTRODUCTION

Measurements of the rate of recombination of electrons with helium ions have spanned a period of twenty years with a generally unsatisfying lack of convergence. Only the results[1–4] of experiments performed under the limiting conditions of low neutral gas pressure and high electron density have been brought into reasonable agreement with theory, as formulated to describe the collisional-radiative recombination[5] of He^+. At higher pressures the variance between measurements has been extreme. Some experiments[6] have indicated no pressure dependence over a range of pressures varying by a factor of 2, while more recent[7] studies show a linear dependence of recombination-rate coefficient on neutral gas pressure.

While the most probable cause of variance has been the stringent experimental criteria which must be met to establish sufficient gas purity, recombination control of loss processes, and the dominance of one type of ion, a group of past measurements remain which are difficult to fault on technique. One such selection of measurements from the literature is shown in Fig. 1, with numbers in parentheses referencing sources.

All cases presented in Fig. 1, with the exception of the lower limit of (1), employed one of several schemes of analysis which required definite *a priori* assumptions to be made about the functional dependence or lack of dependence of the recombination-rate coefficient on experimental parameters such as pressure and electron density. Such assumptions about form have been equivalent to the replacement of the rate coefficient with the first few terms of its power-series expansion. The principal variation in treatment has occurred in the consideration of different degrees of the resulting polynomial. Table I lists the highest

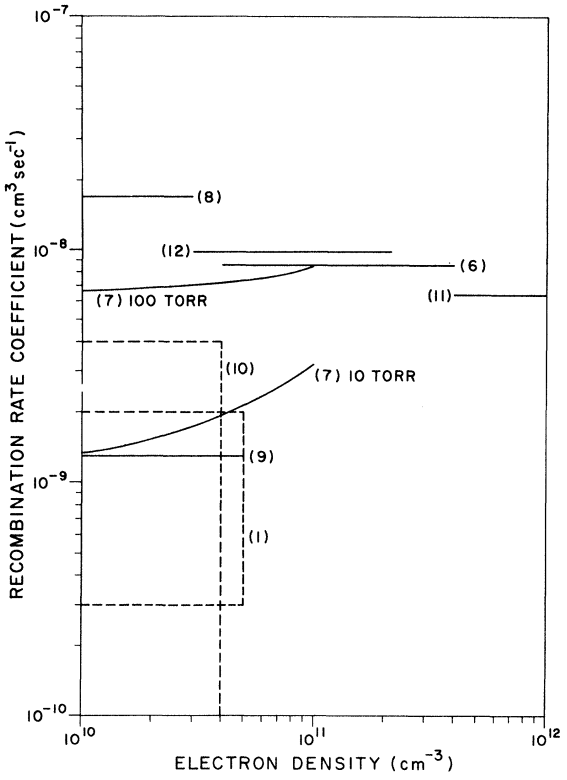

FIG. 1. Graph of selected prior measurements of the recombination-rate coefficient for He_2^+ ions with electrons as functions of electron density. In parentheses is indicated the reference number of source material.

Table I. Summary of the highest degree of polynomial assumed in prior work to represent the dependence in helium at the indicated pressure of the recombination-rate coefficient on electron density and the resulting degree of polynomial found to represent the dependence of rate coefficient on neutral gas density. Dashes indicate measurement over a range of pressures insufficient to indicate the degree of dependence on neutral gas density.

Ref.	Pressure (Torr)	Polynomial degree: Electron density	Polynomial degree: Gas density
1	15	zero	···
6	15–30	zero	zero
7	10–100	one	one
8	21–29	zero	···
9	15–20	zero	···
10	60	zero for upper limit	···
11	100	zero	one
12	15	zero	···

degree assumed to approximate the dependence on electron density for the curves displayed in Fig. 1, together with the degree found to approximate the dependence on neutral gas density over the pressure range examined. In each case, however, unless the resulting polynomial is exact, the coefficients resulting from measurements interpreted under such assumptions must be viewed as a type of weighted average over the range of parameters spanned by the measurement, with different models possibly leading to different weighting methods.

The purpose of this paper is to present the results of a measurement of the recombination-rate coefficient for He_2^+ by a technique which is the logical extension of that used to obtain the lower limit (1) in Fig. 1 and which has been made practicable by the availability of a computer-linked data-acquisition facility.[13] This technique requires no *a priori* knowledge or assumptions of functional form to yield the relative recombination coefficient at specific electron densities. Then from the functional form so measured, scale is established by directly integrating the appropriate rate equation.

METHOD

As discussed by Kerr,[1] a lower limit on the recombination-rate coefficient for ions in an afterglow can be obtained by a bookkeeping technique in which the absolute intensities of radiation in the visible region are summed to determine the rate at which the products of the recombination are being formed at a particular value of experimental parameters. Then, provided that not more than one photon is detected per ion recombined and provided that the relative concentrations of ions and electrons is known, the rate coefficient can be bounded by dividing the recombination rate by the appropriate concentrations as follows:

$$\alpha \geq \textstyle\sum_j I_j/K[e].^{2} \tag{1}$$

Here α is the recombination-rate coefficient for the ion considered at the same particular values of experimental parameters, I_j is the number of photons/sec emitted in all directions per cm^3 from the jth molecular state, $[e]$ is the free-electron concentration, and K is the ratio of the ion to electron concentration.

If it could be established that one and only one photon is detected for each ion recombined, then the expression could be set equal to the rate coefficient. However, when the occurrence of more than one ion is likely, a serious problem develops in the treatment of K, which is quite often a complex function of experimental coordinates. Usually it has been assumed $K=1$ with the consequent restriction upon the range of experimental parameters for which Eq. (1) could be applied. However, an alternative exists as a consequence of the reactions

$$X^+ + e + e \rightleftarrows X^* + e\,, \tag{2}$$

$$X^+ + e + Y \rightleftarrows X^* + Y\,, \tag{3}$$

where the asterisk denotes an excited state. Collins[14] has shown that for states X^* with sufficiently small ionization energy,

$$I_q = C(q, T, T_e)[X^+][e]\,, \tag{4}$$

with

$$C(q, T, T_e) = A_q G(2\pi mKT_e/h^2)^{-3/2} e^{U_q/KT}\,, \tag{5}$$

where I_q is the intensity of radiation from the state X^*, A_q is the transition probability for the emission of this radiation, $[X^+]$ and $[X^*(q)]$ are concentrations of X^+ and the qth excited state of X^*, respectively, G is a combination of relevant statistical weights and partition functions, U_q is the ionization potential for $X^*(q)$, T_e is the electron temperature, and the remaining symbols have conventional meanings except for the distribution temperature T defined elsewhere,[14] for which

$$T_g \leq T \leq T_e\,, \tag{6}$$

with T_g denoting the heavy-particle temperature. Using these expressions, Eq. (1) can be rewritten

$$\alpha = C(q, T, T_e)\textstyle\sum_j I_j/I_q\,. \tag{7}$$

It is useful to collect the assumptions upon which the validity of (7) depends as follows: (a) One and only one photon is detected for each X^+

ion recombined; (b) there is a Rydberg-like series of X^* states and a principal quantum number q which is sufficiently large so that $X^*(q)$ is in collisional equilibrium with the free electrons. In particular, the validity of (7) does not depend on *a priori* knowledge of the functional dependence of α on $[e]$, special simplifications of the continuity equation for charges, the dominance of one particular type of ion, or thermalization of the afterglow. Consequently, if the experimental parameters are changed in such manner that (a) and (b) remain satisfied and either C remains essentially constant or its variation is known, then values of the recombination-rate coefficient can be directly obtained from (7) as functions of the experimental parameters.

Unfortunately, values of A_q are not available for the molecular helium system, so that the rate coefficient for the recombination of the molecular ion He_2^+ in a helium afterglow can in principle be determined without further assumptions only to within a constant scale factor. This scale factor must be determined by one of the several customary techniques, each requiring that at least one of the above additional assumptions be made. The technique most suited to the type of data already available for use in relation (7) is an analysis of the loss rate of ions, which requires a simplification of the continuity equation for He_2^+. If recombination control is assumed and all possible sources of He_2^+ are neglected, as is the usual approximation for a high-pressure helium-afterglow experiment, the rate equation is

$$\frac{d}{dt}[He_2^+] = -\alpha[He_2^+][e]. \tag{8}$$

Integrating this equation, followed by multiplication by $[e]$ and substitution according to (4), yields

$$I_q/C(q, T, T_e) = [e]\int_t^\infty \alpha[X^+][e]\,d\tau. \tag{9}$$

Substituting (4) and then (7) in the integrand and solving the expression for C gives

$$C(q, T, T_e) = I_q\{[e]\textstyle\sum_j \int_t^\infty I_j\,d\tau\}^{-1}. \tag{10}$$

In addition to providing scale for the recombination-rate coefficient, in Eq. (7), this expression is useful in itself to give an indication of the possible change in temperature occurring during the afterglow period.

APPARATUS AND TECHNIQUES

The quartz afterglow cell is shown in Fig. 2. Dual tantalum disks were used as electrodes to produce a uniform high-density plasma. The cell was connected to a high-vacuum system bakeable to 450 °C and capable of ultimate pressures better than 10^{-9} Torr.

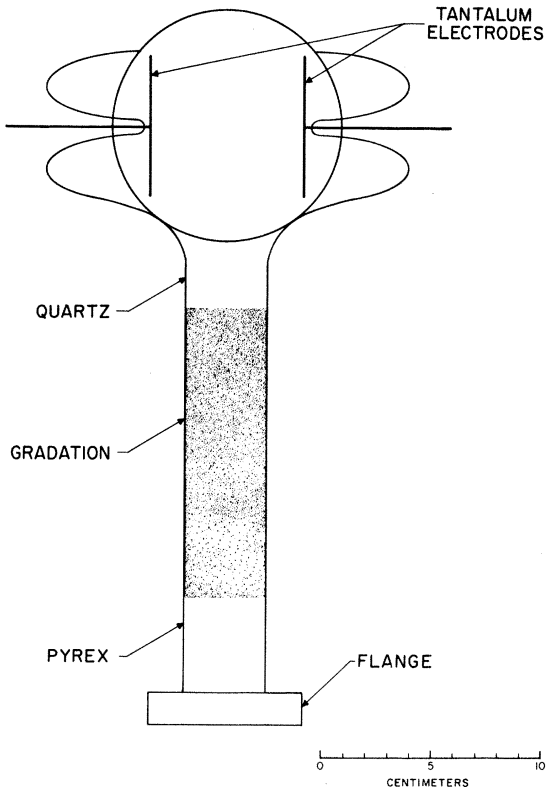

FIG. 2. Scaled drawing of the quartz afterglow cell.

The gas-handling system, operational cycle, instrumentation, and computer-linked data-acquisition system have been discussed in earlier descriptions[4,13] of the University of Texas at Dallas pulsed-afterglow system and were employed with few changes in this experiment. Added to the measurement system was a tandem 0.75-m Czerny-Turner monochromator with gratings blazed for use in the quartz ultraviolet region and resolution set to values between 1 and 10 Å as appropriate to the feature being observed. In addition, the necessity of filling the experimental cell to higher pressures than previously used required that the air-cooled cataphoresis tube for gas purification be replaced with a water-cooled tube.

At the experimental pressure of 44.6 Torr the cell required 5-kV pulses of not greater than 10-μsec duration for dependable operation. Under these conditions the discharge was observed to uniformly fill the region between electrodes. No arcs or constrictions occurred and the discharge appeared quite similar to the beam-excited discharges discussed by Persson.[15]

RESULTS

An examination of the decay of the molecular-

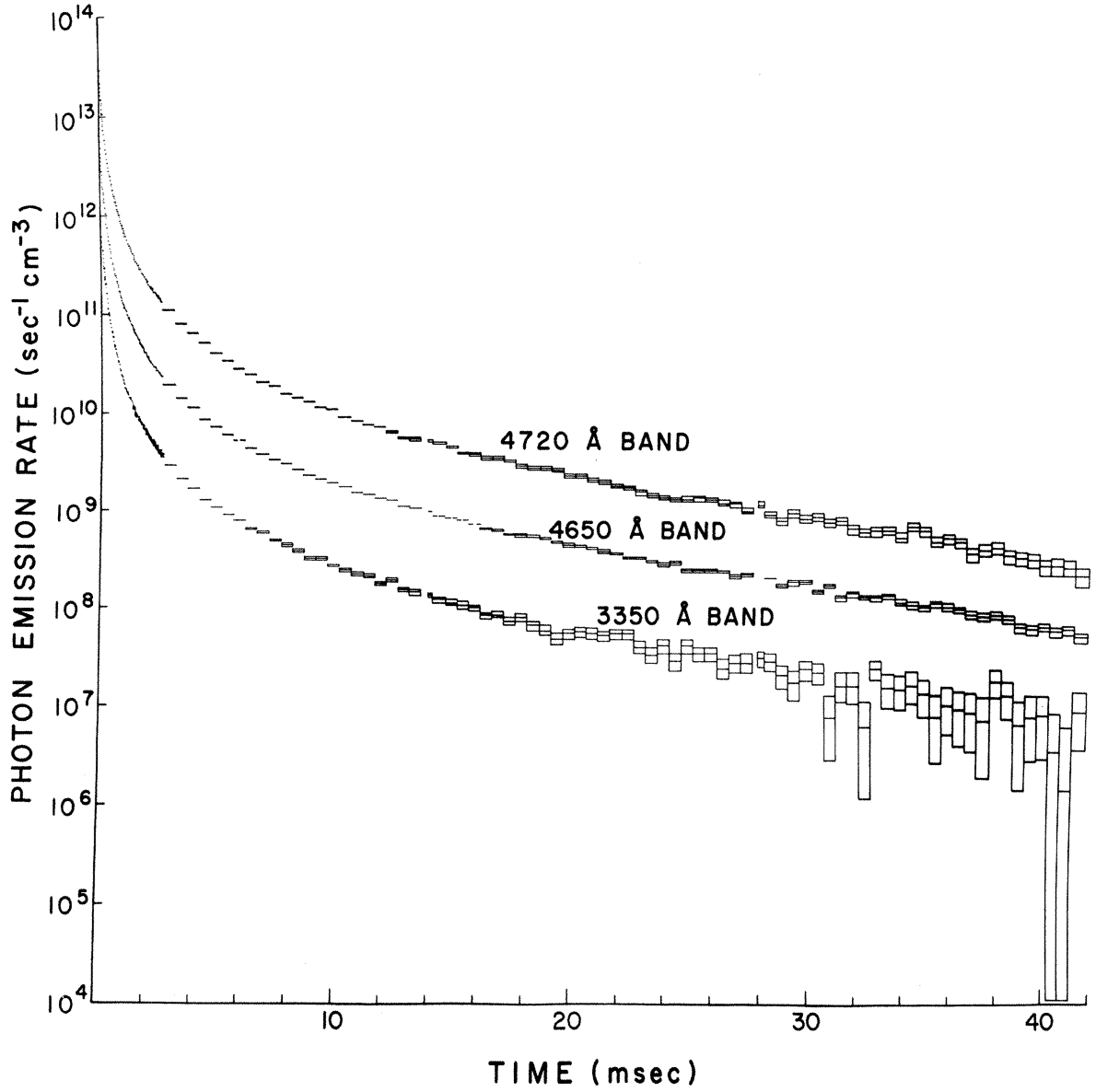

FIG. 3. Graph of the absolute intensities of emission of selected features of the He_2 spectrum as functions of delay time following the initiation of the power pulse. At late times limits are shown representing the data ± standard deviation. Above each curve is the nominal wavelength of the band represented in the graph by the $P(4)$ line of the $4s\,^1\Sigma_u^+ - 2p\,^1\Pi_g$ (4720-Å) band, the $Q(7)$ line of the $3p\,^3\Pi_g - 2s\,^3\Sigma_u^+$ (4650-Å) band, and the $R(1)$ line of the $5p\,^3\Pi_g - 2s\,^3\Sigma_u^+$ (3350-Å) band.

band intensity following the termination of the ionizing pulse showed all visible components to have a common time dependence in agreement with previous observations[1,16,17] of the prominent features of the molecular spectrum. Figure 3 is typical of this observed behavior, illustrating the time dependence of the absolute intensity of the $P(4)$ line of the 4720-Å band ($4s\,^1\Sigma_u^+ - 2p\,^1\Pi_g$), the $Q(7)$ line of the 4650-Å band ($3p\,^3\Pi_g - 2s\,^3\Sigma_u^+$), and the $R(1)$ line of the 3350-Å band ($5p\,^3\Pi_g - 2s\,^3\Sigma_u^+$). Horizontal and vertical dimensions of the data indicate, respectively, the uncertainty in time caused by the finite duration of the sampling interval and the statistical nature of the data. Where possible, the intensity has been plotted together with limits representing the data ± standard deviation.

Extension of these observations was made to other features[18] not previously reported in pulsed-afterglow measurements, such as the 3350- and 4720-Å bands shown in Fig. 3, lines from high rotational states such as the $Q(15)$ of the 4650-Å band and the $R(9)$ of the 5130-Å band ($3p\,^1\Pi_g$

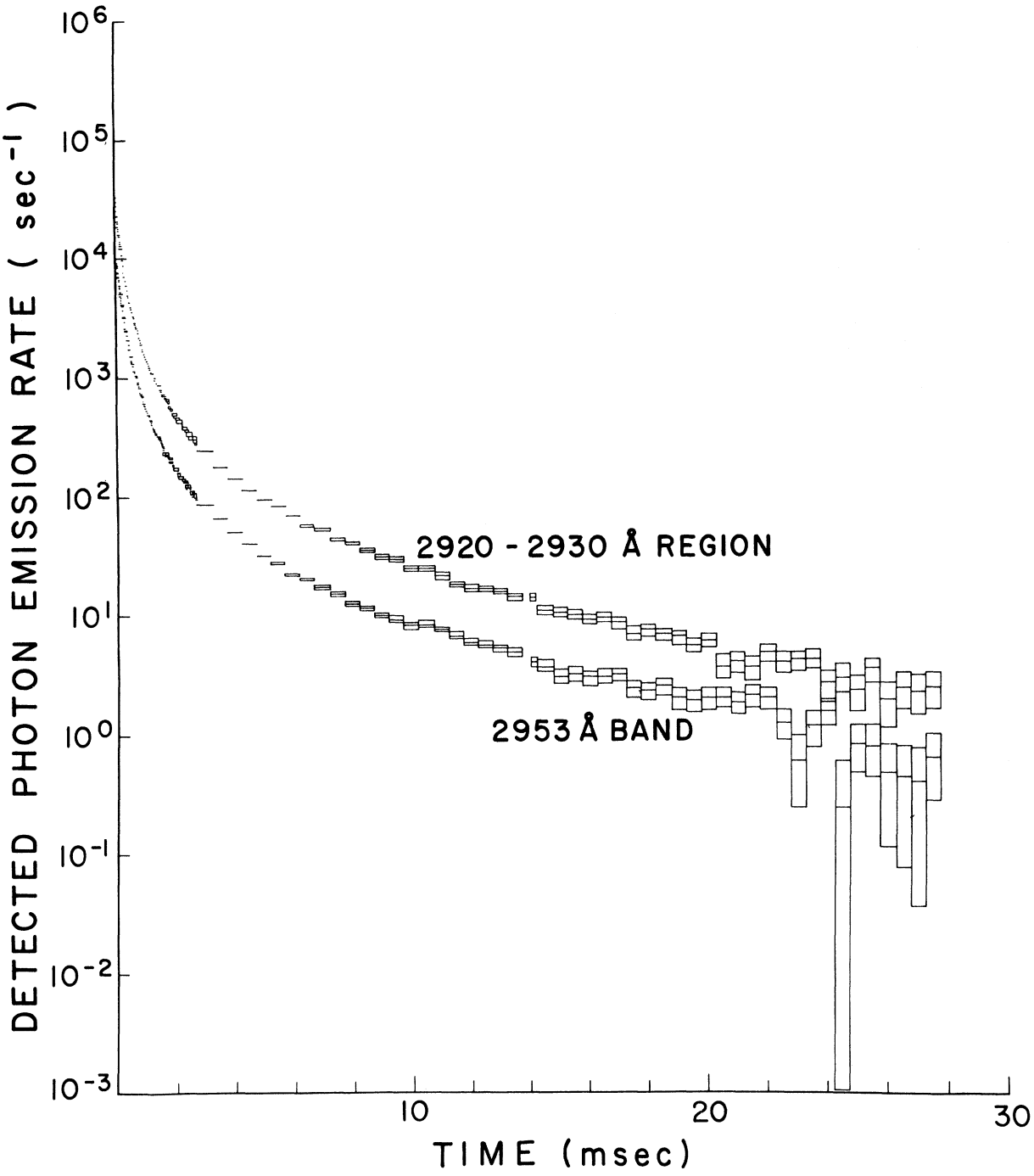

FIG. 4. Graph of the detected photon counting rate as a function of delay time following the initiation of the power pulse for the spectral features of He_2 having the nominal wavelengths indicated. At late times limits are shown representing the data ± standard deviation. The lower curve corresponds to the total intensity of the $16p\,^3\Pi_g - 2s^3\Sigma_u^+$ (2953-Å) band. The upper curve represents the total intensity of the bands and continuum lying within the interval 2920–2930 Å and corresponds to $(\Sigma_{n>24}\, np\,^3\Pi_g - 2s\,^3\Sigma_u^+)$.

$-2s^1\Sigma_u^+$), and bands from vibrationally excited states such as the 4670-Å band ($3p\,^3\Pi_{g,v=1} - 2s^3\Sigma_{u,v=1}^+$). In all cases sampled in the visible region, curves were obtained which were indistinguishable from those of Fig. 3.

Observations in the quartz uv region served to locate the Rydberg series ($np\,^3\Pi_g - 2s\,^3\Sigma_u^+$). Figure 4 presents the results of the measurement of the

band at 2953 Å ($16p\,^3\Pi_g - 2s\,^3\Sigma_u^+$) and the integrated intensity of bands and continuum within the interval 2920–2930 Å ($\sum_{n>24} np\,^3\Pi_g - 2s\,^3\Sigma_u^+$) in terms of the detected photon counting rate as a function of time. Though not apparent in the figure because of the number of orders of magnitude spanned by the data, the functional dependences of both intensities are dissimilar to that of the visible bands of Fig. 3, but common to that found for all high members of the same Rydberg series.

A more useful presentation of the degree of correlation of data of the type shown in Fig. 4 has been found[19] to be a graph of the normalized fractional deviations f defined as

$$f = (I_1 - CI_2)/(I_1 + CI_2) , \qquad (11)$$

where I_1 and I_2 represent the instantaneous intensities of the two spectral features to be compared and C is a normalizing constant generally chosen so that $f = 0$ for the value of time at which deviations are most likely to occur. Then for small changes about zero f is approximately equal to half the fractional change in the separation of the curves. Figure 5 presents the normalized fractional deviations between the intensities plotted in Fig. 4.

ANALYSIS

Parallelism of the curves of Fig. 4 is shown by Fig. 5 to extend to all times examined. This strongly suggests the interpretation that the populations of the upper states radiating these bands are in the type of collisional equilibrium described by Eqs. (4) and (5) with $q \geq 16$.

Referring to Eq. (7), it is then possible to derive from the measured data the relative recombination-rate coefficient as a function of time, and consequently electron density, provided one and only one photon per recombination is represented in the sum of intensities appearing in the numerator of (7). This is a relatively easy condition to establish in principle because radiative deexcitation dominates sufficiently over collisional deexcitation for the lower excited levels of He_2. For example, the rate coefficient calculated[20] for the superelastic deexcitation by electron collisions for

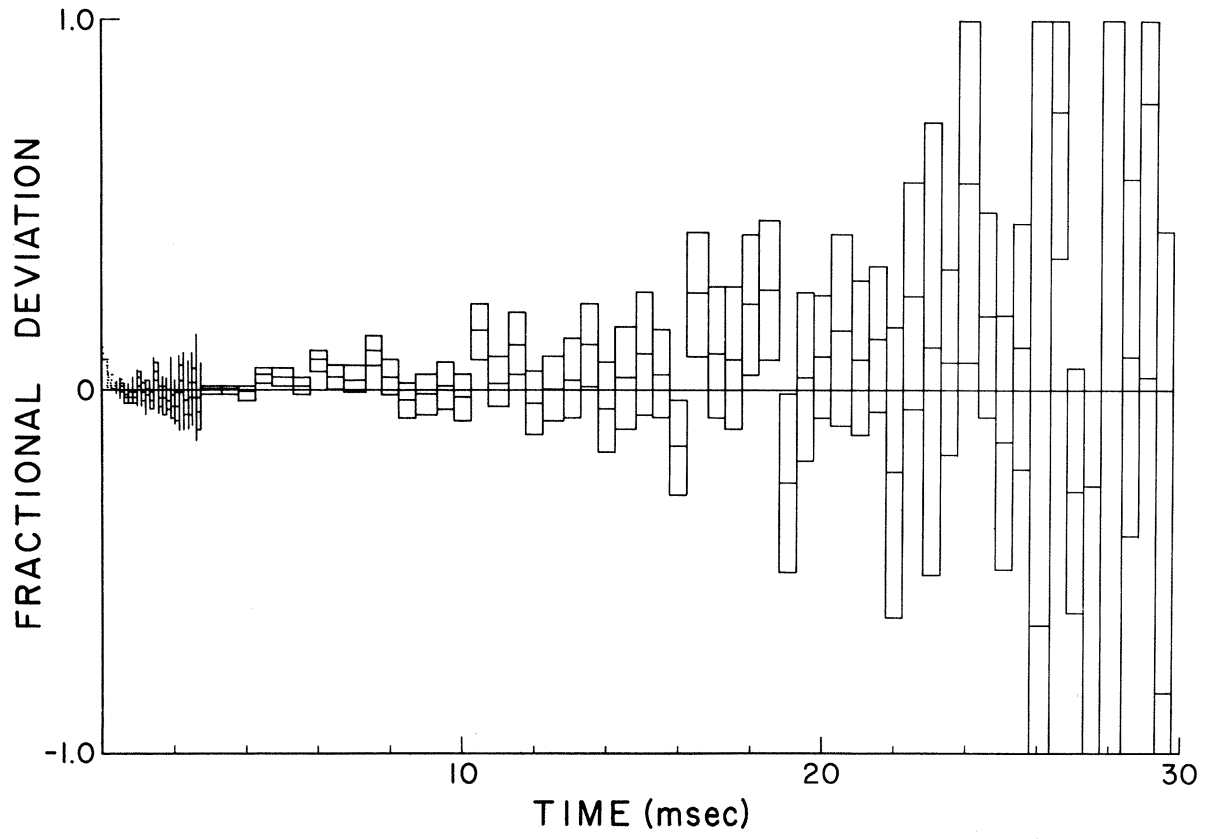

FIG. 5. Graph showing the degree of similarity of functional dependence on time of the intensities of the spectral features plotted in Fig. 4. Ordinates correspond to the normalized fractional difference of the two intensities computed according to Eq. (11).

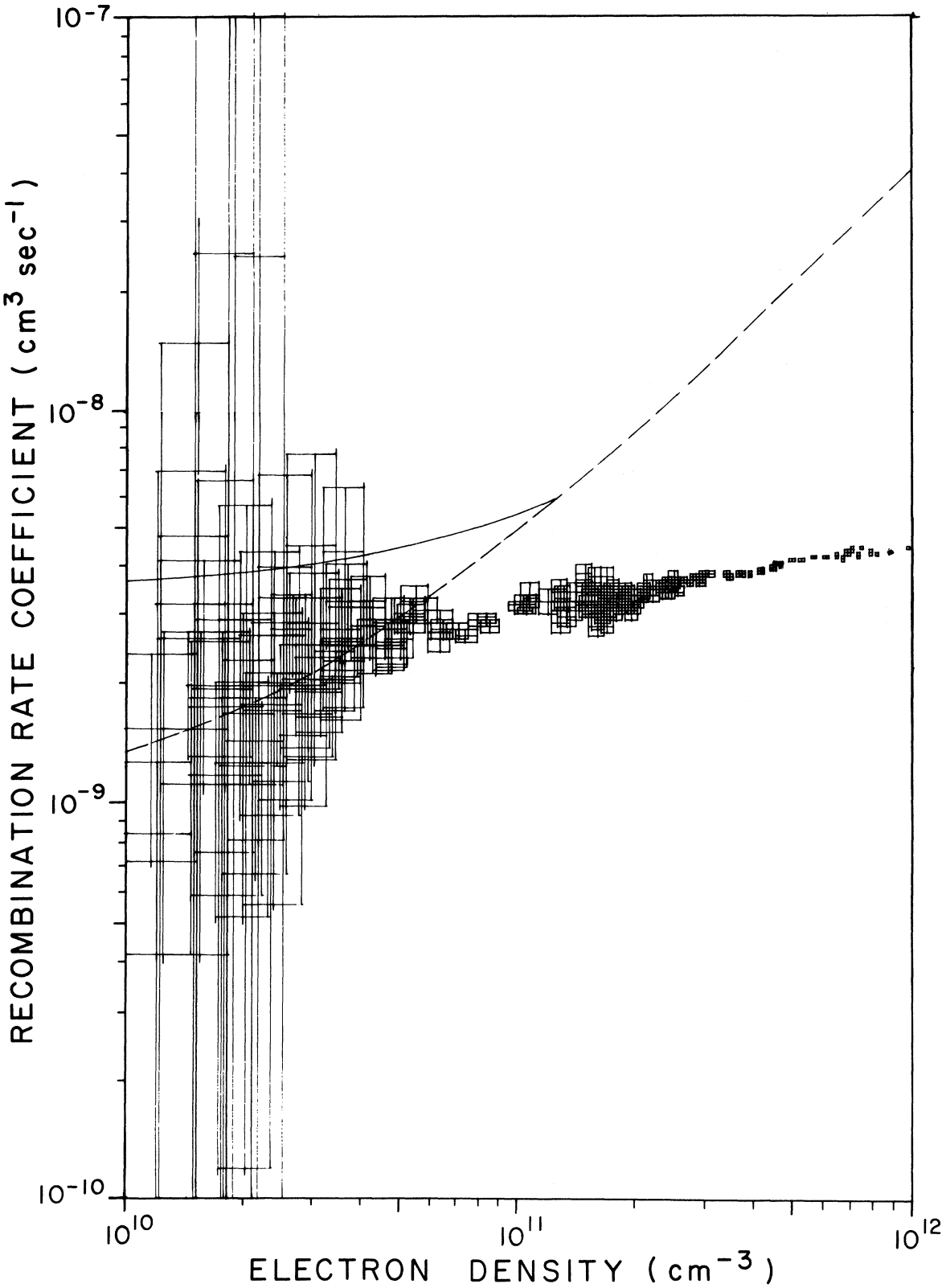

FIG. 6. Graph of the scale function $C'(q, T, T_e)$ as computed from the spectroscopic data according to Eq. (13) and plotted as a function of corresponding electron density. Values are shown as rectangles bounded by the accumulated statistical errors of measurement and including the average values within each.

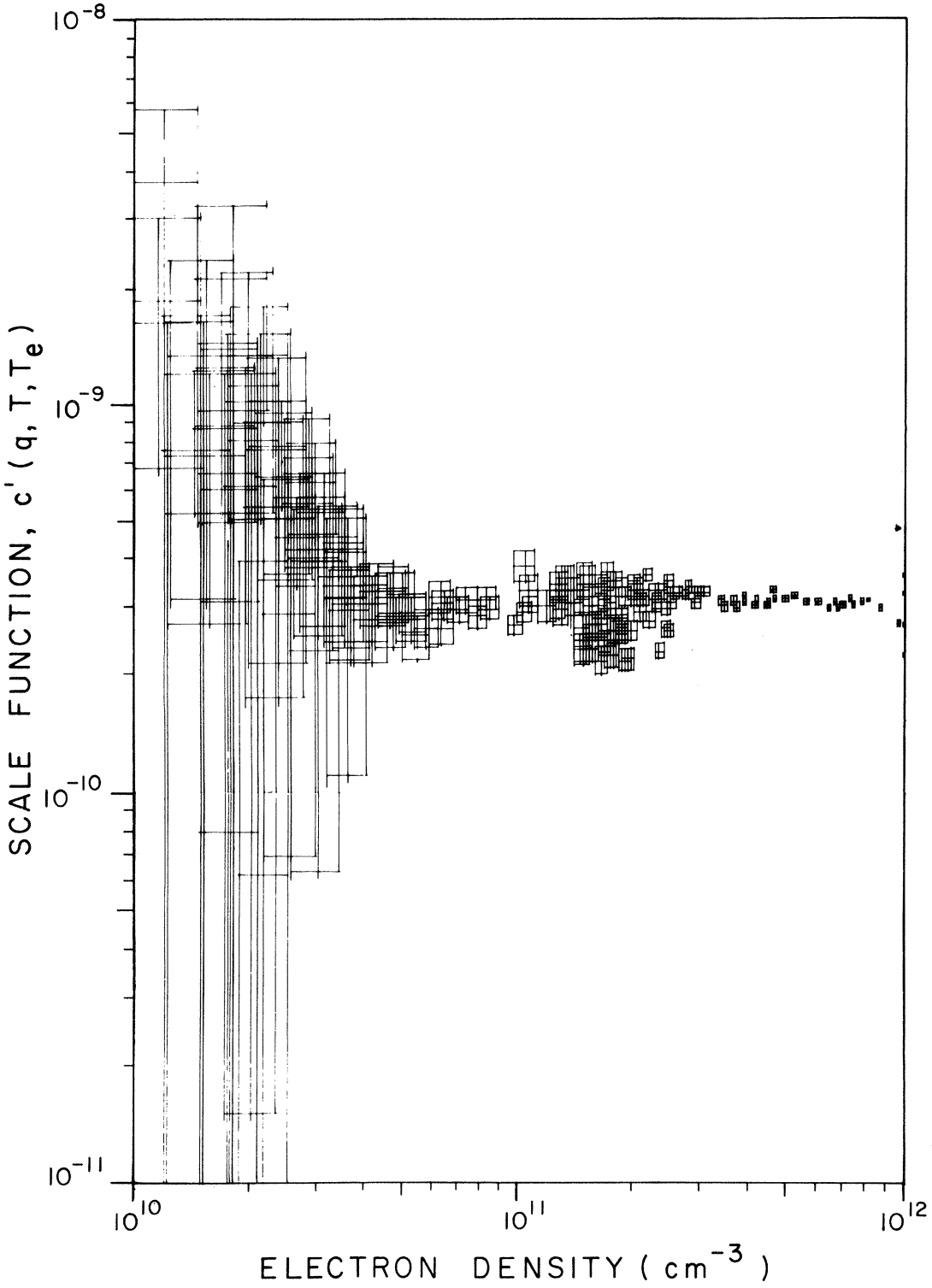

FIG. 7. Graph of rate coefficients for the recombination of He_2^+ ions with electrons as a continuous function of electron density at a neutral helium pressure of 44.6 Torr. The scaled values resulting from this work are shown as rectangles bounded by the accumulated statistical errors of measurement and including the average values within each. For comparison the results interpolated for the same neutral gas pressure from the measurements of the Saclay group (Ref. 7) are plotted without statistical error (solid curve), together with the predictions of theory (dashed curve).

the $n=3$ levels of He_2 is of the order of 6×10^{-9} cm^3/sec, which limits the nonradiative rate of relaxation to a value less than 6×10^3 sec^{-1} at all times in the afterglow. This in comparison with typical radiative rates means that probably less than 1% of the recombining events would be lost by summing only intensities representing transitions to levels with $n\leq2$, where n represents the principal quantum number in the united atom representation of the molecule.

In practice, the computation of the sum of intensities of transitions to levels having $n\leq2$ from levels having $n\geq3$ is facilitated by the fact that all either lie in the wavelength region examined or have upper states which radiate an additional transition which lies in this region. Since all transitions of significant intensity in this wavelength region were found to have constant relative intensities for the duration of the afterglow under the conditions of this experiment, for the purposes of calculating a relative recombination-rate coefficient the numerator of Eq. (7) can be replaced by the intensity I_x of any intense molecular band observed, to give

$$\alpha=C'(q,T,T_e)I_x/I_q. \tag{12}$$

The corresponding change must then be made in expression (10) to give the proper scale function

$$C'(q,T,T_e)=I_q([e]\int_t^\infty I_x\,d\tau)^{-1}. \tag{13}$$

Plotting the data for this scale factor as a function of the average electron density measured with the microwave interferometer[4,13] at each of the corresponding times gave the results shown in Fig. 6. In this figure the cumulative statistical error expected in the scale factor and the uncertainty in electron density give each data block its respective vertical and horizontal dimensions.

The most pronounced feature of the scale function is its lack of apparent dependence on electron density. This suggests a relatively constant electron temperature throughout the afterglow period. Exception must be made, however, for the first 100-μsec period for which the data are badly scattered and for which $[e]>10^{12}$ sec^{-1}.

Using the indicated value of

$$C'(q,T,T_e)=3.1\times10^{-10} \tag{14}$$

for the scale factor and combining data according to expression (12) gave the values, presented in Fig. 7, of the recombination-rate coefficient of He_2^+ with electrons under the conditions of this experiment as a function of electron density. As in the preceding figure, cumulative statistical errors have been shown for each individual measurement.

For comparison the results interpolated from the measurements of the Saclay group[7] for the same neutral gas pressure of 44.6 Torr are shown in Fig. 7 without experimental error, together with the predictions of theory.[7,21] Agreement between experiments can be seen to be quite good over the range of electron densities common to both measurements, 10^{10}–10^{11} cm^{-3}. Since the specific functional form assumed by the Saclay group is not necessarily valid outside the range of parameters over which the coefficients were fitted to the data, the discrepancy between experiments which would result from extrapolation to other values of electron density cannot be considered serious. Conversely, however, there is a serious lack of agreement with the theory of collisional-radiative recombination as applied to He_2^+. As can be seen, the disagreement between theory and both experiments is severe over the common range of measurement and becomes worse at the higher values of electron density. No explanation can be offered at this time, but a reexamination of the theory and particularly the classical cross sections employed appears warranted.

On a strictly empirical basis the functional form

$$\alpha\simeq2.8\times10^{-11}[e]^{0.185}\ cm^3/sec, \tag{15}$$

where $[e]$ is the value of electron density in cm^{-3}, appears to offer the simplest satisfactory approximation to the recombination-rate coefficient of He_2^+ at 44.6 Torr over the range of electron densities spanned by this measurement, 10^{10}–10^{12} cm^3/sec. Although dependent upon simplification of the continuity equation for scale, as are the Saclay results together with most of others shown in Fig. 1, the dependence of rate coefficient on electron density requires only assumptions (a) and (b). In particular,

$$\alpha[C'(q,T,T_e)]\propto[e]^{0.185} \tag{16}$$

requires only that the relatively unrestrictive conditions (a) and (b) be satisfied for validity. The conclusion is indicated that simple polynomial expansions of the recombination-rate coefficient in terms of experimental parameters may be placed in difficulty when large changes in experimental parameters are encountered.

---

*Research supported by the Atmospheric Sciences Section, National Science Foundation, NSF Grant No. GA-15434.

[1]D. E. Kerr, Johns Hopkins University (unpublished);

C. S. Leffel, M. N. Hirsh, and D. E. Kerr (unpublished).
[2]E. Hinnov and J. G. Hirschberg, Phys. Rev. 125, 795 (1962).
[3]R. A. Gerber, G. F. Sauter, and H. J. Oskam, Physica 32, 217 (1966).
[4]C. B. Collins and W. B. Hurt, Phys. Rev. 167, 166 (1968).
[5]D. R. Bates, A. E. Kingston, and R. W. P. McWhirter, Proc. Roy. Soc. (London) A267, 297 (1962).
[6]C. L. Chen, C. C. Leiby, and L. Goldstein, Phys. Rev. 121, 1391 (1961).
[7]R. Deloche, A. Gonfalone, and M. Cheret, Compt. Rend. 267, 934 (1968); J. Berlande, M. Cheret, R. Deloche, A. Gonfalone, and C. Manus, Phys. Rev. A, 1, 887 (1970).
[8]M. A. Biondi and S. C. Brown, Phys. Rev. 75, 1700 (1949).
[9]E. P. Gray and D. E. Kerr, Bull. Am. Phys. Soc. 5, 372 (1960).
[10]H. J. Oskam and V. R. Mittelstadt, Phys. Rev. 132, 1445 (1963).
[11]J. Stevefelt, in Proceedings of the Fourtenth International Conference on Phenomena in Ionized Gases, Bucharest, 1969 (unpublished).
[12]R. A. Johnson, B. T. McClure, and R. B. Holt, Phys. Rev. 80, 376 (1950).
[13]C. B. Collins and W. B. Hurt, Phys. Rev. 177, 257 (1969).
[14]C. B. Collins, Phys. Rev. (to be published).
[15]K. B. Persson, J. Appl. Phys. 36, 3086 (1965).
[16]J. M. Anderson, in *Proceedings of the Fifth International Conference on Ionization Phenomena in Gases, Munich*, 1961, edited by H. Maeckner (North-Holland, Amsterdam, 1962), p. 621.
[17]C. B. Collins and W. W. Robertson, J. Chem. Phys. 40, 2208 (1964).
[18]H. S. Hicks and C. B. Collins, University of Texas at Dallas Report, 1970 (unpublished).
[19]C. B. Collins and W. B. Hurt, Phys. Rev. 179, 203 (1969).
[20]M. Gryzinski, Phys. Rev. 115, 374 (1949).
[21]C. B. Collins, Phys. Rev. 177, 254 (1969).

PHYSICAL REVIEW A VOLUME 2, NUMBER 3 SEPTEMBER 1970

Liouville Energy Eigenvalue Problem

Hsiao S. Kiang

Department of Chemistry, Indiana University, Bloomington, Indiana 47401
(Received 10 February 1970)

The mathematical dilemma of the direct determination of the reduced density matrix for an N-particle system in a stationary state is examined. An energy eigenvalue equation pertaining to the statistical Hamiltonian of a subsystem which determines the reduced density matrix is formulated. It is shown that the construction of this equation represents a classical, semi-quantum-mechanical attitude. The dilemma, in fact, arises from this attitude.

I. INTRODUCTION

The problem at issue in this paper may be termed the "Liouville energy eigenvalue problem." It is concerned with the direct determination of the reduced density matrix of a subsystem contained in a total system which is in a stationary state.

It is an elementary procedure to conceive and derive such an eigenvalue equation. However, the hazards involved in correctly setting up the equation are worth reflection. The attitude adapted in deriving and applying this equation differs notably from that used in the Schrödinger energy eigenvalue problem. The equation incorporates two entirely irreconcilable physical disciplines: It makes contact with quantum-theoretic ingredients on one hand, and on the other, it welds itself into classical, macroscopic concepts. Due to this semiquantum classical origin and the well-known inconsistency between quantum mechanics and classical mechanics, one can see that the above-mentioned difficulties are intrinsic.

We believe that the perplexity and the enormous number of mathematical artifacts generated in the search of an analytical solution to this problem are created because the problem is often stated without adequate exposition of its philosophical background. We do not share the view that the problem could be approached by analytical devices alone.

II. OPERATOR MEAN VALUE

It is easily shown that the mean value of a quantum-mechanical operator of a system of N identical particles,

$$\underline{\Omega}^{(N)} = \sum_{i=1}^{N} \underline{\Omega}(i) + \frac{1}{2!} \sum_{i,j}^{N}{}' \underline{\Omega}(i,j)$$